

Isolated Organometallic Nickel(III) and Nickel(IV) Complexes Relevant to Carbon–Carbon Bond Formation Reactions

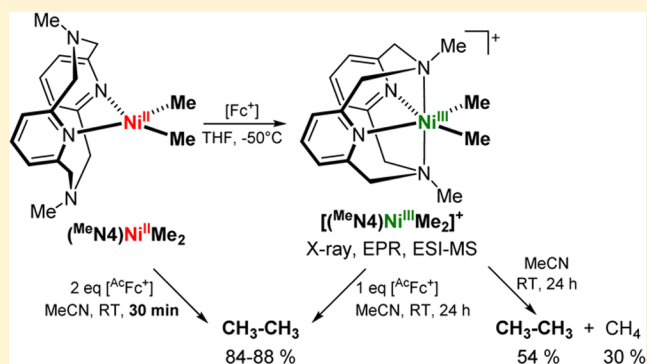
Jason W. Schultz,[†] Kei Fuchigami,[†] Bo Zheng,[†] Nigam P. Rath,[‡] and Liviu M. Mirica^{*,†}

[†]Department of Chemistry, Washington University, One Brookings Drive, St. Louis, Missouri 63130-4899, United States

[‡]Department of Chemistry and Biochemistry, University of Missouri—St. Louis, One University Boulevard, St. Louis, Missouri 63121-4400, United States

S Supporting Information

ABSTRACT: Nickel-catalyzed cross-coupling reactions are experiencing a dramatic resurgence in recent years given their ability to employ a wider range of electrophiles as well as promote stereospecific or stereoselective transformations. In contrast to the extensively studied Pd catalysts that generally employ diamagnetic intermediates, Ni systems can more easily access various oxidation states including odd-electron configurations. For example, organometallic Ni^{III} intermediates with aryl and/or alkyl ligands are commonly proposed as the active intermediates in cross-coupling reactions. Herein, we report the first isolated Ni^{III}–dialkyl complex and show that this species is involved in stoichiometric and catalytic C–C bond formation reactions. Interestingly, the rate of C–C bond formation from a Ni^{III} center is enhanced in the presence of an oxidant, suggesting the involvement of transient Ni^{IV} species. Indeed, such a Ni^{IV} species was observed and characterized spectroscopically for a nickelacycle system. Overall, these studies suggest that both Ni^{III} and Ni^{IV} species could play an important role in a range of Ni-catalyzed cross-coupling reactions, especially those involving alkyl substrates.



INTRODUCTION

Transition metal-catalyzed cross-coupling reactions have become indispensable in the synthesis of a wide range of pharmaceuticals, materials, and fine chemicals.^{1,2} While Pd systems are arguably the most commonly used catalysts in these transformations, Ni-based catalytic systems have been developed recently for cross-coupling reactions given their broader substrate scope and the ability to also employ alkyl electrophiles and nucleophiles.^{3–10} By comparison to the Pd-mediated transformations that generally employ diamagnetic intermediates, the Ni systems can more easily undergo one-electron redox reactions involving Ni^I and Ni^{III} species.^{11–23} For example, a large fraction of Ni-catalyzed cross-coupling reactions are proposed to proceed through organometallic Ni^{III} dialkyl/aryl intermediates that undergo rapid reductive elimination to form a new C–C bond.^{20,24–45} However, to date no such Ni^{III} dialkyl/aryl complexes have been isolated and characterized in detail.

During the past several years, we have employed tetradentate pyridinophane ligands to stabilize uncommon organometallic Pd^{III} and Pd^{IV} complexes capable of C–C and C–heteroatom bond formation reactions.^{46–50} In addition, we have recently used similar ligands to stabilize organometallic Ni^{III} species that can undergo C–heteroatom^{51,52} and C–C bond formation reactions.^{51,53–55} Herein, we employ the ligand *N,N'*-dimethyl-2,11-diaza[3.3](2,6)pyridinophane (^{Me}N4) to stabilize the first

isolated Ni^{III}–dialkyl complex that allowed for its detailed characterization and investigation of its C–C bond formation reactivity. Interestingly, while this Ni^{III} species undergoes C–C bond formation relatively slowly, it undergoes rapid and selective C–C bond formation in the presence of one equivalent oxidant, suggesting the involvement of a transient Ni^{IV} intermediate. Further support for such a species was provided by the isolation of a Ni^{IV} metallacycle complex in which the rate of C–C bond formation is reduced. Overall, these studies report the isolation of Ni^{III}–dialkyl and Ni^{III}–aryl/alkyl complexes and provide strong evidence for the potential involvement of organometallic Ni^{III} and Ni^{IV} species in Ni-catalyzed cross-coupling reactions, especially for transformations involving alkyl substrates.

RESULTS AND DISCUSSION

Synthesis and Characterization of Ni^{III} Complexes.

The red complex (^{Me}N4)Ni^{III}Me₂, **1**, was prepared in 65% yield from the precursor (^{Me}N4)Ni^{II}Br₂ via transmetalation with methylmagnesium chloride (Scheme 1).⁵⁶ The single crystal X-ray structure of **1** reveals a square planar geometry for the Ni center that is bound to two pyridyl nitrogen atoms from the ^{Me}N4 ligand and two methyl groups, with an average equatorial

Received: July 3, 2016

Published: September 6, 2016

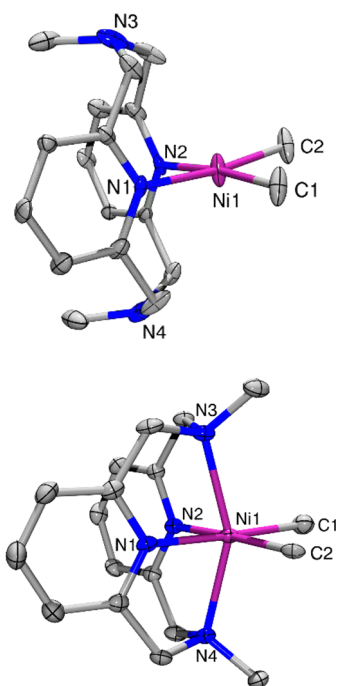
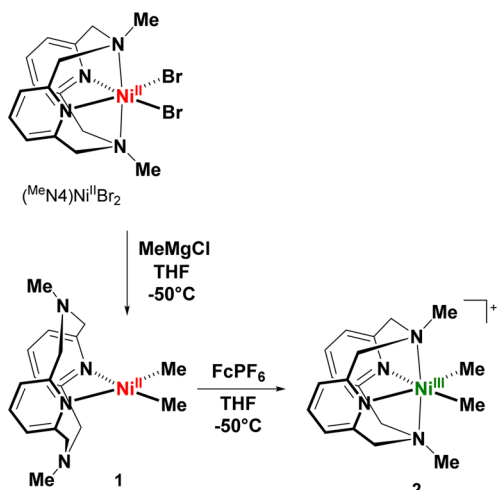
Scheme 1. Synthesis of (^{Me}N4)NiMe₂ Complexes

Figure 1. ORTEP representation of **1** (top) and the cation of **2** (bottom), with 50% probability thermal ellipsoids. Selected bond distances (Å): **1**: Ni1–C1, 1.913; Ni1–C2, 1.913; Ni1–N1, 1.973; Ni1–N2, 1.973; **2**: Ni1–C1, 1.987; Ni1–C2, 1.978; Ni1–N1, 1.979; Ni1–N2, 1.996; Ni1–N3, 2.252; Ni1–N4, 2.240.

Ni–N_{pyridyl} bond length of 1.973 Å and an average Ni–C bond length of 1.913 Å (Figure 1). As expected, **1** is diamagnetic, likely due to the strong σ -donor methyl groups that favor the low-spin square planar geometry. The cyclic voltammetry (CV) of **1** exhibits two oxidation processes at –1500 and –500 mV vs Fc⁺/Fc, as well as a pseudoreversible wave at ~0 V vs Fc⁺/Fc (Figure S1).⁵⁶ The first two oxidation events are tentatively assigned to Ni^{II}/Ni^{III} couples that could correspond to complex **1** in which the ^{Me}N4 ligand adopts different conformations,⁵⁷ while the pseudoreversible oxidation at ~0 V is assigned to a Ni^{III}/Ni^{IV} redox couple (vide infra).

Complex **1** can be easily oxidized with 1 equiv [Cp₂Fe]PF₆ (FcPF₆) in THF at –50 °C to yield [(^{Me}N4)Ni^{III}Me₂]PF₆, **2**, as an orange-red solid.⁵⁶ X-ray quality crystals of **2** were obtained

from THF/pentane, and the crystal structure shows the presence of a Ni^{III} center that adopts a distorted octahedral geometry with an average axial Ni–N_{amine} bond length of 2.246 Å and a shorter average equatorial Ni–N_{pyridyl} bond length of 1.988 Å (Figure 1). These values are consistent with our previously reported organometallic (^RN4)Ni^{III} complexes (Ni–N_{amine} bond lengths of 2.212–2.431 Å, Ni–N_{pyridyl} bond lengths of 1.903–1.965 Å),^{51,53} as well as other reported six-coordinate Ni^{III} complexes.^{58,59} Similarly, an average Ni–C_{Me} bond length of 1.983 Å is consistent with the other structurally characterized Ni^{III}–alkyl complexes reported (1.923, 1.994, 2.011 Å, 2.015, and 2.039 Å).^{60–64} The CV of **2** in MeCN reveals a pseudoreversible oxidation wave at ~0 V vs Fc⁺/Fc, followed by an irreversible oxidation at 0.36 V (Figure S2). The former reversible redox events suggests that the Ni^{IV} oxidation state may be accessible, yet the one-electron oxidized species derived from **2** likely undergoes a rapid chemical reaction such as reductive elimination (vide infra), and the resulting Ni product could give rise to the higher potential irreversible oxidation (i.e., an ECE electrochemical mechanism). The EPR spectrum of complex **2** exhibits a pseudoaxial signal with g_x , g_y , and g_z values of 2.228, 2.210, and 2.014, respectively, and superhyperfine coupling in the g_z direction ($A_{2N} = 14.3$ G) due to the two axial N donors ($I = 1$, Figure 2), consistent with the presence of a

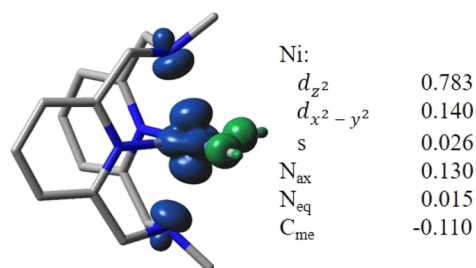
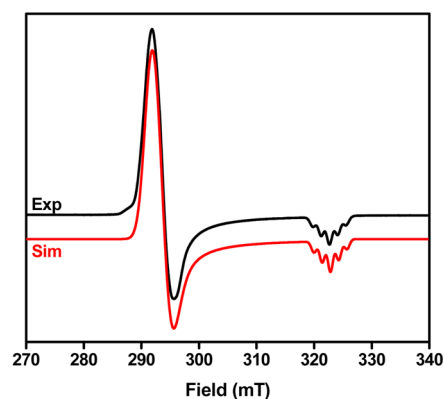


Figure 2. (Top) EPR spectrum (black line) of **2** in PrCN at 77K, and the simulated EPR spectrum (red line) using the following parameters: $g_x = 2.228$, $g_y = 2.210$, $g_z = 2.014$ ($A_{2N} = 14.3$ G). (Bottom) DFT calculated Mulliken spin density for **2** (shown as a 0.05 isodensity contour plot), and the relevant atomic and Ni orbital contributions to the spin density.

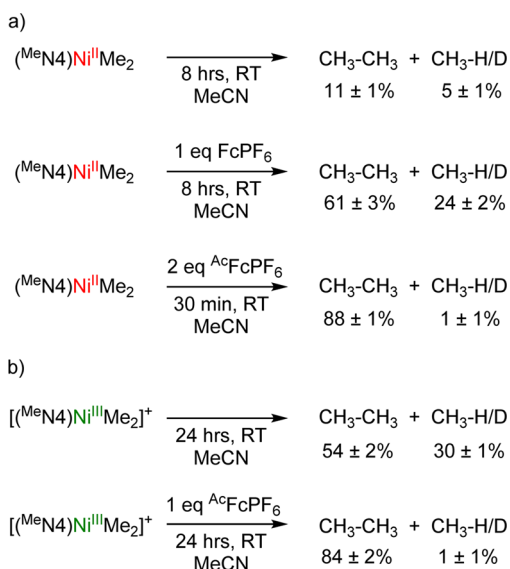
Ni^{III} metal center in a d_z^2 ground state.^{22,58,59,65,66} Furthermore, density functional theory (DFT) calculations and the calculated spin density support a metal-based radical description for **2** in which the unpaired electron resides mostly on the Ni center (Figure 2). Importantly, **2** represents to the best of our knowledge the first isolated Ni^{III}–dialkyl complex. With this compound in hand, we can now probe directly its reactivity, especially since

such organometallic Ni^{III} species have been proposed for the past few decades as key intermediates in cross-coupling and other C–C bond formation reactions.^{24–45}

C–C Bond Formation Reactivity of Ni^{III/II} Complexes.

The organometallic reactivity of **1** and **2** was then investigated under different reaction conditions. First, a solution of **1** in MeCN slowly generates ethane in 11% yield in 8 h at room temperature under N₂, along with a detectable amount of methane (Scheme 2a). The reductive elimination of ethane

Scheme 2. C–C Bond Formation Reactivity of the (Me₄N)NiMe₂ Complexes

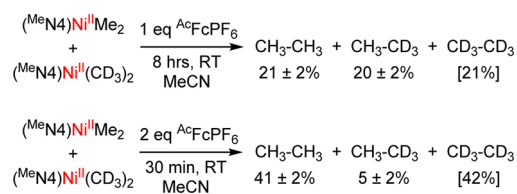


from **1** most likely proceeds through a classical Ni^{II}/Ni⁰ mechanism, as suggested by the formation of an observable amount of Ni black. While performing the reductive elimination at elevated temperatures does lead to formation of ethane in larger yields, appreciable amounts of methane were also observed; thus, all reactivity studies were performed at RT to limit the side reactions. By comparison, the addition of 1 equiv of a mild oxidant such as ferrocenium hexafluorophosphate (FcPF₆) or acetylferrocenium hexafluorophosphate (^{Ac}FcPF₆) to a solution of **1** under N₂ increases the ethane yield to 61% in 8 h, yet methane is also produced in 24% yield. Interestingly, addition of 2 equiv ^{Ac}FcPF₆ to a solution of **1** in MeCN resulted in clean formation of ethane in 88% yield in 30 min at RT under N₂ (Scheme 2a). Since the oxidation potential of ^{Ac}FcPF₆ (~0.25 V vs Fc⁺/Fc)⁶⁷ is more positive than the potential corresponding to the reversible oxidation observed for **1** and tentatively assigned to the Ni^{III}/Ni^{IV} redox couple (vide supra), the rapid formation of ethane suggests the involvement of a Ni^{IV} intermediate. The C–C bond formation reactivity of the isolated Ni^{III} complex **2** was also probed, to reveal that **2** in MeCN slowly generates 54% ethane after 24 h, along with an appreciable amount of methane (Scheme 2b). By comparison, addition of 1 equiv ^{Ac}FcPF₆ to a solution of **2** in MeCN afforded ethane cleanly in 84% yield after 24 h, further supporting the potential involvement of a Ni^{IV} species in the ethane elimination step (Scheme 2b). The slower reactivity observed for **2** in the presence of 1 equiv ^{Ac}FcPF₆ vs that of **1** in the presence of 2 equiv ^{Ac}FcPF₆ is proposed to be due to the 6-coordinate geometry of the Ni^{III} center in **2**, a geometry expected to be maintained in a Ni^{IV} species, which should

undergo reductive elimination slower than a 4- or 5-coordinate Ni^{IV} species generated upon direct two-electron oxidation of the square planar Ni^{II} complex **1**.^{68,69} For all these reactivity studies proposed to involve high-valent Ni species, the final Ni product was determined to be the paramagnetic species $[(\text{Me}_4\text{N})\text{Ni}^{\text{II}}(\text{MeCN})_2]^{2+}$, which could be crystallized out of the reaction mixture.⁵⁶

Additional mechanistic studies were employed to probe the observed C–C bond formation reactivity. Crossover experiments employing a 1:1 mixture of **1** and (Me₄N)Ni^{II}(CD₃)₂, **1-d**₆, in MeCN revealed that upon addition of 1 equiv ^{Ac}FcPF₆ a 1:1 mixture of CH₃CH₃ and CH₃CD₃ was generated in ~20% yield for each product after 8 h (Scheme 3). Given the typical

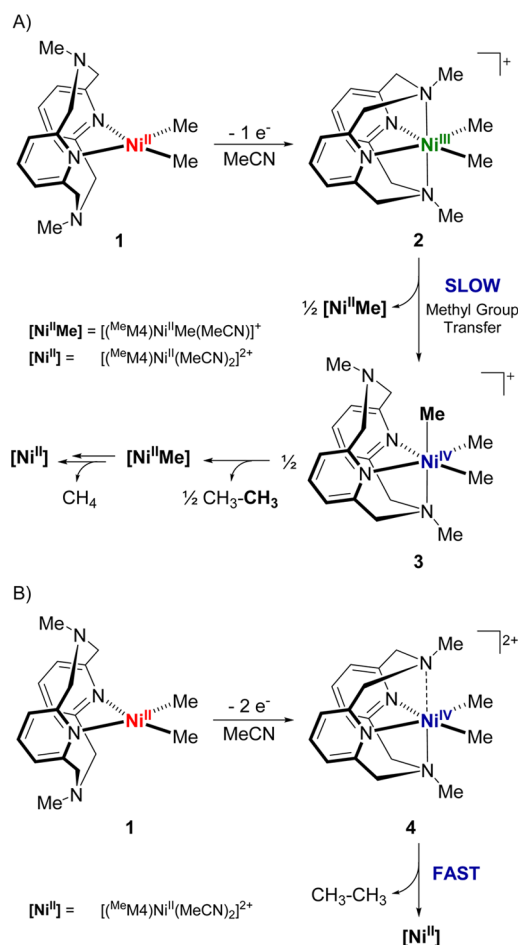
Scheme 3. Crossover Reactivity Studies of (Me₄N)Ni^{II}Me₂



yield of ~60% ethane upon one-electron oxidation of **1** under the same conditions, the result suggests a CH₃CH₃/CH₃CD₃/CD₃CD₃ ratio of 1:1:1. By comparison, the addition of 2 equiv ^{Ac}FcPF₆ to a 1:1 mixture of **1** and (Me₄N)Ni^{II}(CD₃)₂, **1-d**₆, in MeCN rapidly generates in 30 min ~40% CH₃CH₃ along with a very small amount of CH₃CD₃ (Scheme 3). Given the typical yield of 88% ethane upon two-electron oxidation of **1**, this result suggests that almost no crossover occurs under these conditions, to give a CH₃CH₃/CH₃CD₃/CD₃CD₃ ratio of 1:~0:1, while the small amount (<5%) of CH₃CD₃ detected most likely arises from transient formation of **2** through partial one-electron oxidation of **1**. Importantly, the yields of ethane under all of the investigated conditions are not affected significantly in the presence of the radical trap 2,2,6,6-tetramethylpiperidine-1-oxyl (TEMPO) and no TEMPO-Me was detected,⁵⁶ suggesting that no free methyl radicals are formed in the reaction mixture.

Based on the reactivity studies mentioned above, two different mechanisms are proposed for the observed C–C bond formation reactions. The slower ethane formation reactivity observed upon one-electron oxidation of the Ni^{II} complex **1**, or even slower when starting from the isolated Ni^{III} complex **2**, is proposed to proceed through a methyl group transfer step that would require the dissociation of one of the amine N donors, thus limiting the reaction rate (Scheme 4A). Such a slow methyl group transfer between two Ni centers is supported by the formation of the ethane products CH₃–CH₃/CH₃–CD₃/CD₃–CD₃ in a 1:1:1 ratio, and is similar to our analogous high-valent Pd systems that have been investigated in detail.^{46–48} Formation of a transient $[(\text{Me}_4\text{N})\text{Ni}^{\text{IV}}\text{Me}_3]^+$ intermediate **3** is then expected to undergo reductive elimination of ethane (Scheme 4A). By comparison, the two-electron oxidation of the Ni^{II} complex **1** or one-electron oxidation of the isolated Ni^{III} complex **2** is proposed to directly generate a reactive dicationic $[(\text{Me}_4\text{N})\text{Ni}^{\text{IV}}\text{Me}_2]^{2+}$ species **4** that should rapidly generate ethane upon reductive elimination (Scheme 4B). In this case, no appreciable crossover ethane products should be generated, unless a small fraction of the Ni^{II} precursor is only partially oxidized to the Ni^{III} complex **2**. The rate of ethane formation should be particularly increased when

Scheme 4. Proposed Mechanisms for One-Electron (A) and Two-Electron (B) Oxidation of 1 and Subsequent C–C Bond Formation (the Bold Methyl Group in 3 Represents an Isotopically Labeled Group That Could Lead to Crossover Products)

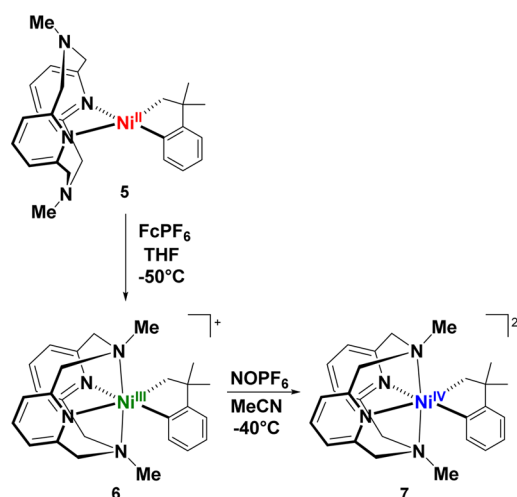


the square planar Ni^{II} complex **1** is rapidly oxidized by two electrons, as that could generate a transient and more reactive 4- or 5-coordinate Ni^{IV} species formed before the conformation change of the ^{Me}N4 ligand to become a tetradentate ligand.⁴⁸ This is also supported by the CV of **1** (Figure S1) that reveals two oxidation events assigned to the Ni^{II}/Ni^{III} couple that corresponds to two conformations of the ^{Me}N4 ligand binding in a tridentate and bidentate fashion to the Ni center, respectively, and similarly to what was observed previously for analogous Pd complexes.⁵⁷ In addition, we cannot exclude the possibility that methyl group exchange could occur at the Ni^{II} center in **1**. However, if such methyl exchange is rapid, the formation of a statistical mixture of (^{Me}N4)Ni^{II}(CH₃)₂/^{(Me}N4)Ni^{II}(CH₃)(CD₃)/(^{Me}N4)Ni^{II}(CD₃)₂ in a 1:2:1 ratio is expected, which upon reductive elimination would generate a 1:2:1 mixture of CH₃–CH₃/CH₃–CD₃/CD₃–CD₃, which was not observed experimentally. Finally, particularly surprising is the limited reactivity of the isolated Ni^{III} complex **2**, although several previous studies of Ni-catalyzed cross-coupling reactions have proposed Ni^{III} dihydrocarbyl species as the key intermediates undergoing rapid C–C bond formation.^{24–45} While the limited reactivity of **2** could be due to the use of a tetradentate ligand that generates a coordinatively saturated Ni center, it may be important to consider that in some Ni systems

an increased C–C bond formation reactivity could be due to the formation of reactive transient Ni^{IV} species. This may be especially relevant to alkyl–alkyl cross-coupling transformations, as the presence of two strong σ -donor alkyl groups on the Ni center should facilitate the formation of a Ni^{IV} species under catalytic conditions.^{8,70,71}

Synthesis and Characterization of a Ni^{IV} Complex. In order to provide further evidence for the proposed Ni^{IV} species **4** mentioned above, we set out to synthesize a more stable Ni^{IV} species supported by the ^{Me}N4 ligand. Previously, use of the cycloneophyl group (–CH₂CMe₂-*o*-C₆H₄–) has been shown to limit the extent of C–C reductive elimination from Ni^{IV} and Pd^{IV} intermediates.^{15,17,72–76} As such, the red complex (^{Me}N4)Ni^{II}(cycloneophyl), **5**, was prepared in 63% yield from the (PMe₃)₂Ni^{II}(cycloneophyl) precursor⁷⁷ via ligand exchange with ^{Me}N4 (Scheme 5),⁵⁶ and its single crystal X-ray structure

Scheme 5. Synthesis of (^{Me}N4)Ni(cycloneophyl) Complexes 6 and 7



reveals a square planar geometry for the Ni^{II} center with an average equatorial Ni–N_{pyridyl} bond length of 1.967 Å and an average Ni–C bond length of 1.917 Å (Figure 3), similar to the bond lengths observed for **1**. In addition, the CV of **5** shows well-defined oxidation waves at –1.17 and 0.25 V vs Fc⁺/Fc, which are assigned to the Ni^{II}/Ni^{III} and Ni^{III}/Ni^{IV} redox couples, respectively. Indeed, oxidation of **5** with 1 equiv FcPF₆ in THF at –50 °C produces [(^{Me}N4)Ni^{III}(cycloneophyl)]PF₆, **6**, as an orange solid in 79% yield (Scheme 5). The Ni^{III} center in **6** adopts a distorted octahedral geometry with an average axial Ni–N_{amine} bond length of 2.254 Å and a shorter average equatorial Ni–N_{pyridyl} bond length of 1.999 Å. As for the Ni–C bond lengths, the Ni–C_{sp3} bond is slightly longer than the Ni–C_{sp2} bond (1.973 Å vs 1.920 Å), as observed previously for other high-valent Ni and Pd(cycloneophyl) complexes.^{72,74–76} Similarly to **2**, the EPR spectrum of **6** exhibits a pseudoaxial signal with observable superhyperfine coupling in the *g_z* direction (*A_N* = 14.5 G).⁵⁶

Importantly, the reversible redox event present in the CV of **6** at *E*_{1/2} = 0.21 V vs Fc⁺/Fc suggests that the corresponding Ni^{IV} complex should be accessible, and oxidation of **6** with 1 equiv NOPF₆ in MeCN at –40 °C yielded the desired orange-red complex [(^{Me}N4)Ni^{IV}(cycloneophyl)](PF₆)₂, **7** (Scheme 5). While several attempts to structurally characterize **7** were unsuccessful, the complex was fully characterized by 1D and 2D

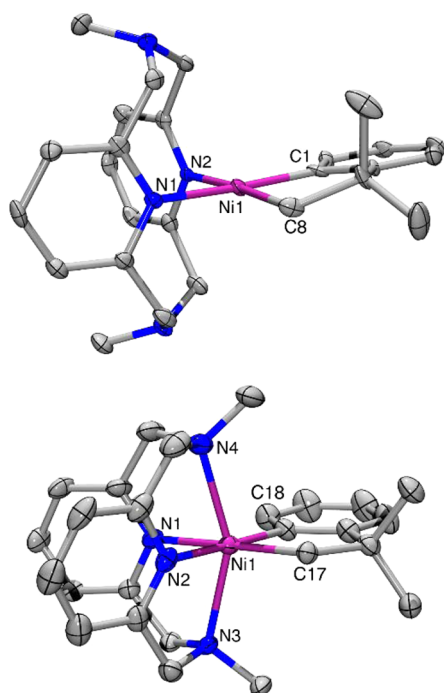


Figure 3. ORTEP representation of **5** (top) and the cation of **6** (bottom) with 50% probability thermal ellipsoids. Selected bond distances (Å): **5**: Ni1–C1, 1.879; Ni1–C8, 1.954; Ni1–N1, 1.936; Ni1–N2, 1.997; **6**: Ni1–C17, 1.973; Ni1–C18, 1.920; Ni1–N1, 2.001; Ni1–N2, 1.997; Ni1–N3, 2.241; Ni1–N4, 2.266.

$^1\text{H}/^{13}\text{C}$ NMR (Figures S12–S17), which reveal significantly downfield shifted resonances for **7** compared to **5** and suggest the presence of a more oxidized metal center.⁵⁶ The downfield shift is most notable for the methylene protons of the cycloneophyl group that move from 1.24 ppm in **5** to 5.33 ppm in **7**. In addition, the presence of a Ni^{IV} center was confirmed by X-ray photoelectron spectroscopy (XPS), which shows an increase of the Ni $2_{p_{3/2}}$ and $2_{p_{1/2}}$ binding energies of ~ 0.6 eV between **6** and **7** and is consistent with the presence of a more oxidized Ni center in **7** vs **6** (Figure 4).⁷⁸ The use of the cycloneophyl bidentate ligand does indeed limit the rate of reductive elimination from both **6** and **7**, as the 1,1-

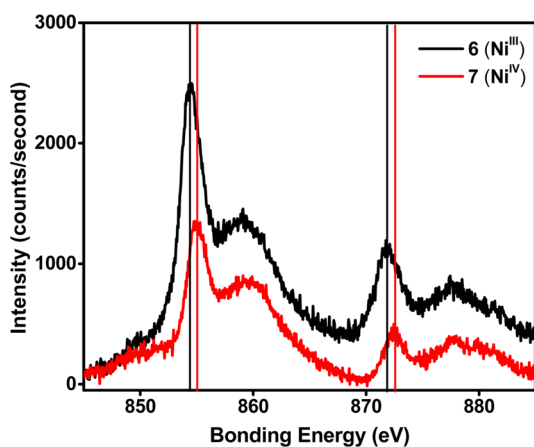


Figure 4. X-ray photoelectron spectra of the Ni binding energy region for complexes **6** (black line) and **7** (red line). Selected bonding energies (eV): **6**: $2_{p_{3/2}}$ 854.43; $2_{p_{1/2}}$ 871.79; **7**: $2_{p_{3/2}}$ 854.97; $2_{p_{1/2}}$ 872.46.

dimethylbenzocyclobutane product was obtained in only 10% and 38% yield, respectively, after 48 h at RT.⁵⁶ Overall, these results confirm the formation of a Ni^{IV} complex supported by the $^{\text{Me}}\text{N}4$ ligand and provide strong support for the potential involvement of Ni^{IV} species in the oxidatively induced C–C bond formation reactions described above. Finally, it is important to note that the $^{\text{Me}}\text{N}4$ ligand system supports the formation of Ni complexes in three different oxidation states (II, III, and IV) and thus could be employed in comparative reactivity studies aimed at deciphering the role of each oxidation state in various organometallic reactions, especially those relevant to cross-coupling reactions.

Catalytic Reactivity of Ni Complexes. In addition to stoichiometric C–C bond formation studies, we have also investigated the ability of the $(^{\text{Me}}\text{N}4)\text{Ni}$ complexes to catalyze cross-coupling reactions. Gratifyingly, **1** was shown to be an active catalyst for the Kumada coupling of aryl iodides with aryl or alkyl Grignard reagents. For example, the reaction of iodotoluene with phenylmagnesium bromide or 1-hexylmagnesium bromide affords the corresponding coupled products in 96% and 60% unoptimized yields, respectively, in 1 h at RT (Scheme 6). In addition, the reaction of chlorotoluene with phenylmagnesium bromide yields the coupled product in 62% yield, although longer reaction time were needed for full conversion. By contrast, the coupling of 1-iodooctane with 1-hexylmagnesium bromide yielded only 20% of the coupled product (Scheme 6).⁵⁶

Scheme 6. Kumada Cross-Coupling Reactions Catalyzed by **1**^a

R-X + R'-MgBr		5% $(^{\text{Me}}\text{N}4)\text{NiMe}_2$		THF, RT		R-R'	
R-X	R'MgX	Time, h	Yield ^a				
<i>p</i> -tolyl-I	PhMgBr	1	96 %				
<i>p</i> -tolyl-Cl	PhMgBr	24	62 %				
<i>p</i> -tolyl-I	hexylMgBr	1	60 %				
octyl-I	hexylMgBr	1	20 %				

^aYields were determined using GC-FID with decane as the internal standard; no coupled products were observed in these reactions in the absence of **1**.⁵⁶

The reduced catalytic reactivity of **1** observed in the presence of an alkyl halide was further probed in a stoichiometric reaction. Addition of CD_3I to **1** in MeCN led to rapid formation of the Ni^{III} species **2**, as observed by EPR (Scheme S22), followed by its slow decay and formation of ethane in 67% yield after 24 h, along with 20% CD_3CH_3 (Scheme 7). When the reaction of **1** with CD_3I was performed in the presence of the radical trap TEMPO, the TEMPO- CD_3 adduct was detected by GC in 85% yield and thus confirming the formation of CD_3^\bullet radicals in the reaction mixture (Scheme 7).⁵⁶ This result provides strong support for the ability of alkyl halides to undergo single-electron transfer (SET) from the Ni^{II} complexes and generate high-valent Ni intermediates, as proposed previously in several mechanistic studies of Ni-catalyzed cross-coupling reactions.^{34,51,79} In the absence of the

- (29) Phapale, V. B.; Guisan-Ceinos, M.; Bunuel, E.; Cardenas, D. J. *Chem. - Eur. J.* **2009**, *15*, 12681.
- (30) Gong, H. G.; Gagné, M. R. *J. Am. Chem. Soc.* **2008**, *130*, 12177.
- (31) Vechorkin, O.; Hu, X. *Angew. Chem., Int. Ed.* **2009**, *48*, 2937.
- (32) Vechorkin, O.; Proust, V. r.; Hu, X. *J. Am. Chem. Soc.* **2009**, *131*, 9756.
- (33) Everson, D. A.; Shrestha, R.; Weix, D. J. *J. Am. Chem. Soc.* **2010**, *132*, 920.
- (34) Biswas, S.; Weix, D. J. *J. Am. Chem. Soc.* **2013**, *135*, 16192.
- (35) Joshi-Pangu, A.; Wang, C. Y.; Biscoe, M. R. *J. Am. Chem. Soc.* **2011**, *133*, 8478.
- (36) Yu, X. L.; Yang, T.; Wang, S. L.; Xu, H. L.; Gong, H. G. *Org. Lett.* **2011**, *13*, 2138.
- (37) Dai, Y. J.; Wu, F.; Zang, Z. H.; You, H. Z.; Gong, H. G. *Chem. - Eur. J.* **2012**, *18*, 808.
- (38) Xu, H.; Zhao, C.; Qian, Q.; Deng, W.; Gong, H. *Chem. Sci.* **2013**, *4*, 4022.
- (39) Aihara, Y.; Tobisu, M.; Fukumoto, Y.; Chatani, N. *J. Am. Chem. Soc.* **2014**, *136*, 15509.
- (40) Tellis, J. C.; Primer, D. N.; Molander, G. A. *Science* **2014**, *345*, 433.
- (41) Zuo, Z. W.; Ahneman, D. T.; Chu, L. L.; Terrett, J. A.; Doyle, A. G.; MacMillan, D. W. C. *Science* **2014**, *345*, 437.
- (42) Tasker, S. Z.; Jamison, T. F. *J. Am. Chem. Soc.* **2015**, *137*, 9531.
- (43) Huihui, K. M. M.; Caputo, J. A.; Melchor, Z.; Olivares, A. M.; Spiewak, A. M.; Johnson, K. A.; DiBenedetto, T. A.; Kim, S.; Ackerman, L. K. G.; Weix, D. J. *J. Am. Chem. Soc.* **2016**, *138*, 5016.
- (44) Qin, T.; Cornella, J.; Li, C.; Malins, L. R.; Edwards, J. T.; Kawamura, S.; Maxwell, B. D.; Eastgate, M. D.; Baran, P. S. *Science* **2016**, *352*, 801.
- (45) Cornella, J.; Edwards, J. T.; Qin, T.; Kawamura, S.; Wang, J.; Pan, C. M.; Gianatassio, R.; Schmidt, M.; Eastgate, M. D.; Baran, P. S. *J. Am. Chem. Soc.* **2016**, *138*, 2174.
- (46) Khusnutdinova, J. R.; Rath, N. P.; Mirica, L. M. *J. Am. Chem. Soc.* **2010**, *132*, 7303.
- (47) Khusnutdinova, J. R.; Rath, N. P.; Mirica, L. M. *J. Am. Chem. Soc.* **2012**, *134*, 2414.
- (48) Tang, F.; Qu, F.; Khusnutdinova, J. R.; Rath, N. P.; Mirica, L. M. *Dalton Trans.* **2012**, *41*, 14046.
- (49) Tang, F.; Zhang, Y.; Rath, N. P.; Mirica, L. M. *Organometallics* **2012**, *31*, 6690.
- (50) Mirica, L. M.; Khusnutdinova, J. R. *Coord. Chem. Rev.* **2013**, *257*, 299.
- (51) Zheng, B.; Tang, F.; Luo, J.; Schultz, J. W.; Rath, N. P.; Mirica, L. M. *J. Am. Chem. Soc.* **2014**, *136*, 6499.
- (52) Zhou, W.; Schultz, J. W.; Rath, N. P.; Mirica, L. M. *J. Am. Chem. Soc.* **2015**, *137*, 7604.
- (53) Tang, F. Z.; Rath, N. P.; Mirica, L. M. *Chem. Commun.* **2015**, *51*, 3113.
- (54) Zhou, W.; Rath, N. P.; Mirica, L. M. *Dalton Trans.* **2016**, *45*, 8693.
- (55) Zhou, W.; Zheng, S. A.; Schultz, J. W.; Rath, N. P.; Mirica, L. M. *J. Am. Chem. Soc.* **2016**, *138*, 5777.
- (56) See the [Supporting Information](#).
- (57) Khusnutdinova, J. R.; Rath, N. P.; Mirica, L. M. *Inorg. Chem.* **2014**, *53*, 13112.
- (58) Grove, D. M.; van Koten, G.; Mul, W. P.; Vanderzeijden, A. A. H.; Terheijden, J.; Zoutberg, M. C.; Stam, C. H. *Organometallics* **1986**, *5*, 322.
- (59) van de Kuil, L. A.; Veldhuizen, Y. S. J.; Grove, D. M.; Zwikker, J. W.; Jenneskens, L. W.; Drenth, W.; Smeets, W. J. J.; Spek, A. L.; van Koten, G. *J. Organomet. Chem.* **1995**, *488*, 191.
- (60) Pandarus, V.; Zargarian, D. *Chem. Commun.* **2007**, 978.
- (61) Castonguay, A.; Beauchamp, A. L.; Zargarian, D. *Organometallics* **2008**, *27*, 5723.
- (62) Lee, C. M.; Chen, C. H.; Liao, F. X.; Hu, C. H.; Lee, G. H. *J. Am. Chem. Soc.* **2010**, *132*, 9256.
- (63) Lipschutz, M. I.; Yang, X.; Chatterjee, R.; Tilley, T. D. *J. Am. Chem. Soc.* **2013**, *135*, 15298.
- (64) Lipschutz, M. I.; Tilley, T. D. *Angew. Chem., Int. Ed.* **2014**, *53*, 7290.
- (65) Grove, D. M.; van Koten, G.; Zoet, R.; Murrall, N. W.; Welch, A. J. *J. Am. Chem. Soc.* **1983**, *105*, 1379.
- (66) Grove, D. M.; van Koten, G.; Mul, P.; Zoet, R.; van der Linden, J. G. M.; Legters, J.; Schmitz, J. E. J.; Murrall, N. W.; Welch, A. J. *Inorg. Chem.* **1988**, *27*, 2466.
- (67) Connelly, N. G.; Geiger, W. E. *Chem. Rev.* **1996**, *96*, 877.
- (68) Crumpton, D. M.; Goldberg, K. I. *J. Am. Chem. Soc.* **2000**, *122*, 962.
- (69) Racowski, J. M.; Sanford, M. S. *Top. Organomet. Chem.* **2011**, *35*, 61.
- (70) Aihara, Y.; Chatani, N. *J. Am. Chem. Soc.* **2013**, *135*, 5308.
- (71) Aihara, Y.; Chatani, N. *J. Am. Chem. Soc.* **2014**, *136*, 898.
- (72) Qu, F.; Khusnutdinova, J. R.; Rath, N. P.; Mirica, L. M. *Chem. Commun.* **2014**, *50*, 3036.
- (73) Perez-Temprano, M. H.; Racowski, J. M.; Kampf, J. W.; Sanford, M. S. *J. Am. Chem. Soc.* **2014**, *136*, 4097.
- (74) Camasso, N. M.; Perez-Temprano, M. H.; Sanford, M. S. *J. Am. Chem. Soc.* **2014**, *136*, 12771.
- (75) Racowski, J. M.; Gary, J. B.; Sanford, M. S. *Angew. Chem., Int. Ed.* **2012**, *51*, 3414.
- (76) Camasso, N. M.; Sanford, M. S. *Science* **2015**, *347*, 1218.
- (77) Carmona, E.; Gutierrezpuebla, E.; Marin, J. M.; Monge, A.; Paneque, M.; Poveda, M. L.; Ruiz, C. *J. Am. Chem. Soc.* **1989**, *111*, 2883.
- (78) Colpas, G. J.; Maroney, M. J.; Bagyinka, C.; Kumar, M.; Willis, W. S.; Suib, S. L.; Baidya, N.; Mascharak, P. K. *Inorg. Chem.* **1991**, *30*, 920.
- (79) Breitenfeld, J.; Ruiz, J.; Wodrich, M. D.; Hu, X. *J. Am. Chem. Soc.* **2013**, *135*, 12004.